# Microstructure evolution of the Gleeble-simulated heat-affected zone of Ni-based superalloy

*Łukasz* Rakoczy[1,*], *Fabian* Hanning[2], *Joel* Andersson[3], *Małgorzata* Grudzień-Rakoczy[4], *Rafał* Cygan[5], and *Anna* Zielińska-Lipiec[1]

[1]AGH University of Science and Technology, Faculty of Metals Engineering and Industrial Computer Science, Mickiewicza 30, 30-059 Krakow, Poland
[2]Chalmers University of Technology, Department of Industrial and Materials Science, 41296 Gothenburg, Sweden
[3]University West, Department of Engineering Science, Gustava Melins Gata 2, 46132 Trollhättan, Sweden
[4]Lukasiewicz Research Network-Foundry Research Institute, Zakopianska 73, 30-418 Krakow, Poland
[5]Consolidated Precision Products Corporation, Investment Casting Division, Hetmanska 120, 35-078 Rzeszow, Poland

**Abstract.** The formation of liquation cracking in a simulated heat affected zone of René108 is reported. The stress controlled thermo-mechanical experiments were carried out on a Gleeble®3800 testing system. The base alloy was lost-wax cast and then solution treated and aged. Light and scanning electron microscopy of this material revealed high volume fraction of γ' precipitates in the dendrite arms and residual eutectic γ/γ' islands in the interdendritic areas. As a result of short-term exposure to high homologous temperature, the volume fraction of γ' phase was significantly decreased due to the dissolution of precipitates in the surrounding matrix. The thin non-equilibrium liquid film, formed locally along grain boundaries, was a key-factor favoring initiation of cracks and their spreading during the Gleeble testing. The liquid appeared as a result of constitutional liquation, mainly of the γ' precipitates.

## 1 Introduction

The combination of high mechanical properties and resistance to hot corrosion make cast Ni-based superalloys one of the most important materials in the construction of jet engine components. Their mechanical properties of alloys are mainly dependent on the morphology, size, distribution and volume fraction of γ' precipitates. The intermetallic $Ni_3Al$ phase has good crystallographic matching with the γ matrix; lattice misfit is generally below one percent [1]. This is also connected with a low coarsening rate of precipitates during service. The crystallographic relationship is represented by: {100} γ//{100} γ', <010> γ//<010> γ'. Ordering is connected with the strictly defined location of Ni and Al atoms in the crystal lattice, which influences further behavior during deformation. The intermetallic phase is very rigid and impedes dislocation movement from the matrix, thus resulting in the required strength. By selecting appropriate technological parameters during casting and heat treatment, a microstructure favorable for the expected service temperature of the jet engines can be attained [2, 3]. Service conditions often cause premature failure of components due to hot corrosion and LCF (low cycle fatigue) cracking. The high cost of parts makes repair welding technologies relevant. It is well-known that precipitation hardened superalloys are susceptible to hot cracking during welding and strain age cracking upon postweld heat treatment [4-6]. Reduced weldability is

caused by considerable content of γ'-formers (above 6% wt. Al + Ti). Cracking is usually observed in heat affected zone and occurs by constitutional liquation phenomena, firstly investigated by Pepe and Savage [7]. The necessary condition for the occurrence of constitutional liquation in Ni-based superalloys is the presence of intermetallic phases, carbides, or topologically closed packed phases at a temperatures equal to or exceeding the eutectic temperature during heating above the solvus line [8].

## 2 Material and methodology

Examination of hot ductility of Ni-based superalloy widely known as René 108 was performed by the computer controlled Gleeble® 3800 device. The experiment was carried out at the Production Technology Center of the University West in Sweden. Chemical composition of the superalloy obtained by optical emission spectroscopy is (%wt): Cr-11.4, Co-8.8, W-8.2, Al-6.4, Ta-3.6, Hf-1.5, Ti-0.8, Mo-0.5, C-0.08, B-0.015, Ni-Bal. The material was a conventionally cast and have subjected to full heat treatment: solution (1200 ˚C) and ageing (900 ˚C) in a vacuum furnace. During experiments, the typical characteristics for hot ductility test (Fig. 1) were recorded, namely Nil Ductility Temperature (NDT), Ductility Recovery Temperature (DRT) and the Nil Strength Temperature (NST). The NST was determined, by using a constant load (0.08

---
* Corresponding author: lrakoczy@agh.edu.pl

kN), to measure the temperature when the material cannot sustain any load.
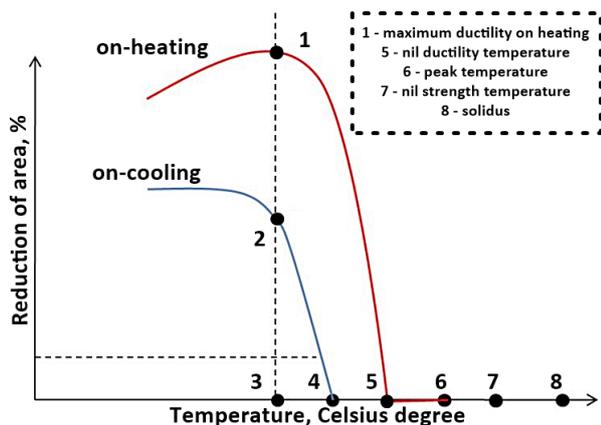


**Fig. 1.** Scheme of Gleeble study [9].

Metallographic preparation of samples included grinding, polishing and electrochemical etching in 10 % oxalic reagent. The microstructure was examined by scanning electron microscopy (SEM) on a Phenom XL instrument equipped with an Energy dispersive X-ray spectrometer.

# 3 Results and discussion

## 3.1 Microstructure of base alloy

The microstructure showed significant local microsegregation of the chemical composition (Fig. 2). The material was characterized by a very complex chemical composition when compared to the majority of popular superalloys.
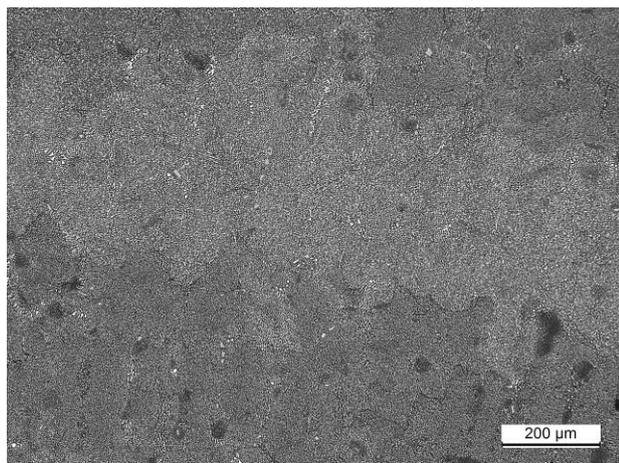


**Fig. 2.** Dendritic structure of equiaxed Ni-based superalloy René 108.

The high content of alloying elements and their limited solubility in the γ phase led to the formation of numerous microstructural constituents. Relatively homogeneous dendrite arms structure within which the fine

intermetallic phase precipitates were surrounded by γ channels.
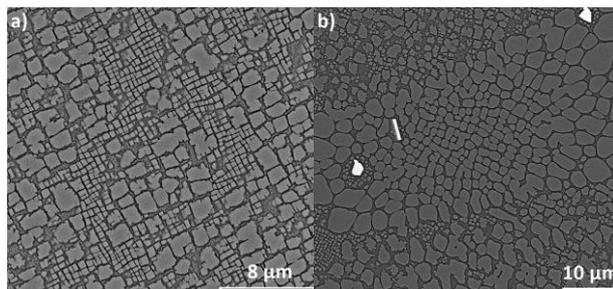


**Fig. 3.** Morphology of γ' precipitates: a) dendrite arm; b) interdendritic space.

The size of precipitates in interdendritic spaces was incomparably larger, and their morphology was much more complex (Fig. 3). Despite the similar content of γ'-formers in the various nickel superalloys, the contribution of eutectic islands in the microstructure can vary within a wide range, which can be exemplified by René 108 and for example IN713C [2].
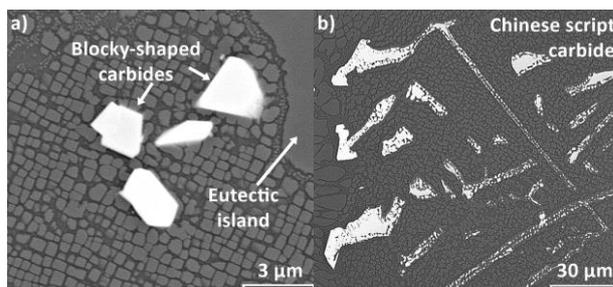


**Fig. 4.** Morphology of strengthening phases: a) carbides surrounded by cubic-shaped γ' precipitates; b) Chinese script carbide.

Carbide formers segregated to interdendritic spaces (Fig. 4). Inside the eutectic islands, as well as in their close vicinity, numerous carbides with a morphology of blocks, parallelograms and a typical Chinese script pattern have been noticed.

## 3.2 Microstructural degradation of Gleeble-simulated heat affected zone

The temperature at which the nickel superalloy was characterized by zero strength, namely NST, was equal to 1290 °C. The microstructure of a cross-section of the sample after exposure to this temperature is shown in Fig. 5. Numerous precipitates on the edge of the crack indicated that they was initiated and then propagating along interdendritic spaces. The morphology of the constituents at the edge of the crack indicated that during Gleeble test constitutional liquation mainly of the γ' phase along grain boundaries took place. A significant volume of carbides also dissolved in the matrix.
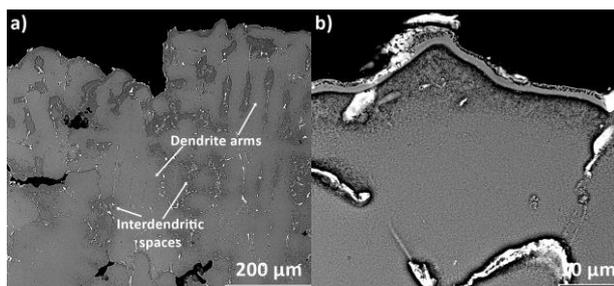
**Fig. 5.** Degraded microstructure of simulated HAZ: a) location of crack, dendrite arms and interdendritic spaces;
b) re-solidified products and precipitates along edge of crack.

During cooling after rupture of the sample, the liquid re-solidified through the eutectic transformation. Nickel crystallizes in the face-centered cubic crystal structure, and so eutectic γ/γ' grew epitaxially towards <100> direction [1]. In the close vicinity of the fracture, eutectic islands γ/γ' were melted while the gamma prime and carbides strongly were dissolved.
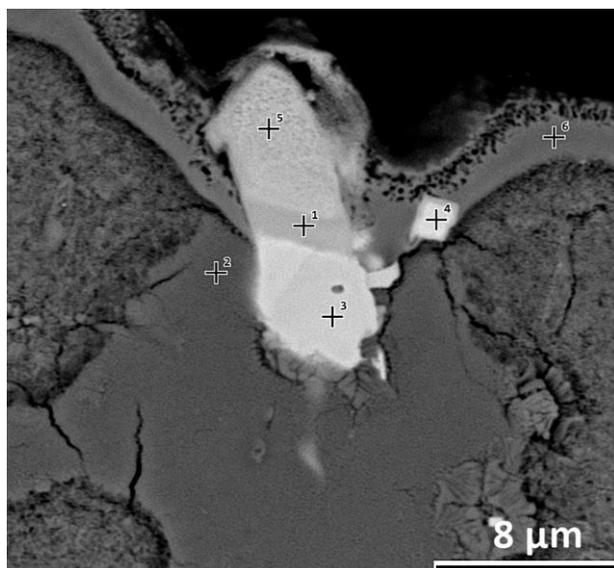


**Fig. 6.** Location of EDS analysis points.

Elements affecting the weldability of Ni-based superalloys include also minor elements like carbon, boron, sulfur. Precipitates at the edge of the crack were subjected to quantitative EDS microanalysis (Fig. 6). The results collected from 6 areas are shown in Table 1. Measurements in points 1, 3, 4 and 5 indicated the presence of MC type carbide enriched in Hf and Ta. The relationship Hf to Ta was in the range 1.73-2.42. In the base material, borides enriched in tungsten were also observed, hence its increased content in points 1 and 3 may be the result of the dissolution of borides. Boron decreases local melting point and thus increase susceptibility to liquation cracking [4]. Measurement no. 2 was carried out in the eutectic island γ/γ', as indicated by the increased concentration of Al. The last measurement showed the chemical composition of the re-solidified layer formed from the non-equilibrium liquid film.

**Table 1.** Results of EDS analysis in location 1-6 (%at.)

| Point Element | 1 | 2 | 3 | 4 | 5 | 6 |
|---|---|---|---|---|---|---|
| **Hf** | 51.2 | | 45.2 | 44.8 | 52.3 | |
| **Ta** | 25.8 | | 25.3 | 25.9 | 21.6 | |
| **W** | 9.4 | 4.1 | 7.4 | | 2.4 | 4.5 |
| **Ni** | 6.3 | 63.6 | 6.7 | 12.4 | 6.2 | 67.6 |
| **Ti** | 5.9 | 1.6 | 5.6 | 3.1 | 4.3 | 0.6 |
| **Co** | 1.4 | 7.0 | | 2.4 | 1.6 | 9.8 |
| **Al** | | 20.0 | 9.8 | 9.9 | 10.8 | 10.1 |
| **Cr** | | 3.7 | | 1.5 | 0.8 | 7.4 |

## 4 Summary

The investigated superalloy was characterized by a considerable microstructural heterogeneity, which had a significant influence on varied microstructural degradation in dendrite arms and cores in comparison with interdendritic spaces. The primary and secondary γ' precipitates in the dendrite cores and arms were almost completely dissolved in the matrix during the tests and subsequently re-precipitated during cooling as nanometric precipitates. The presence of numerous strengthening phases in interdendritic spaces, namely carbides, borides, and eutectic islands lead to much larger microstructural degradation in these areas. The high heating rate during the Gleeble test created favourable conditions for the non-equilibrium reactions, including constitutional liquation. Microstructural observations indicated that a liquid phase appeared along the grain boundaries in the HAZ and locally in close vicinity of MC-type carbides. The morphology of the re-precipitation products allowed us to deduce their formation process.

## References

1. R. Reed, The superalloys: Fundamentals and Applications, (Cambridge University Press, Cambridge, 2006)

2. Ł. Rakoczy, R. Cygan, Arch. Civ. and Mech. Eng., **18**, 4 (2018).
   https://doi.org/10.1016/j.acme.2018.05.008

3. Ł. Rakoczy et al., Inter. J. Mat. Research **110**, 1 (2019) https://doi.org/10.3139/146.111729

4. Ł. Rakoczy et al., Arch. Met. Mat. 63, 1 (2018) DOI: 10.24425/118926

5. F. Hanning, J. Andersson, Weld World, 62, 1 (2017) https://doi.org/10.1007/s40194-017-0508-z

6. F. Hanning, J. Andersson, The influence of base metal microstructure on weld cracking in manually GTA repair welded cast ATI 718plus®, Proceedings

of the 9th International Symposium on Superalloy 718 & Derivatives: Energy, Aerospace, and Industrial Applications. The Minerals, Metals & Materials Series, Springer (2018) https://doi.org/10.1007/978-3-319-89480-5_61

7. J. Pepe, W. Savage, Weld. J., 49 (1970)

8. J.N. Dupont et al., Welding metallurgy and Weldability of Nickel-Base Alloys (John Wilay&Sons, Inc., Hoboken, New Jersey, 2009)

9. ISO/TR 17641-3:2005. Destructive tests on welds in metallic materials -- Hot cracking tests for weldments -- Arc welding processes -- Part 3: Externally loaded tests